Plate Boundary Adjustments of the Southernmost Queen Charlotte Fault

by Kristin M. M. Rohr

Abstract   A revision of the plate boundary configuration offshore southern Haida Gwaii, which is the locus of the 2012 M_w 7.8 thrust earthquake, is based on a re-evaluation of regional geophysical data and leads to recognition of fault segments critical for seismic-hazard analysis. Off western Canada, the strike-slip Queen Charlotte fault (QCF) and Revere–Dellwood fault (RDF) constitute the transpressive plate boundary between the Pacific and North American plates. The southernmost 80 km of the QCF strikes at the highest angle (∼20°) to the relative plate motion, yet geomorphology adjacent to the fault is the most subdued. Synthesizing geomorphology, seismicity, sidescan sonar, gravity, and seismic reflection profiles indicates that the plate boundary is evolving to a less transpressive configuration than previously interpreted. The RDF is 100 km longer than previously mapped; it has propagated northward and overlaps the QCF by 120 km. Propagation is defined by strike-slip earthquakes $3.9 < M_w < 6.4$, 500 m uplift of oceanic crust, and a fault scarp that disrupts margin parallel structures of the Queen Charlotte terrace. Part of the southern QCF has been reoriented through a series of short restraining steps, resulting in a less oblique orientation relative to the plate motions; the recent fault trace is clearly seen in previously uninterpreted sidescan sonar data. Overall this mapping delineates a segment of the plate boundary characterized by overlap between the QCF and RDF and defines the southern limit of a segment of the plate boundary characterized by historic pure shear deformation and rupture during the 2012 M_w 7.8 and the 1949 **M** 8.1 earthquakes.

Introduction

After a change in relative plate motion, strike-slip plate boundaries tend to evolve toward more efficient configurations, that is, the principal deformation zone becomes aligned with the new relative plate motion vector (Wilcox *et al.*, 1973). A change in plate motions at 5–6 Ma put the plate boundary between the Pacific and North American plates (Atwater and Stock, 1998; Doubrovine and Tarduno, 2008) offshore western Canada (Fig. 1) into varying degrees of transpression. Strike-slip motion between these two plates is largely carried by the Queen Charlotte fault (QCF); its strike differs by 20°–5° from current plate motions from the southern tip of Haida Gwaii to the Alaska–British Columbia border (Rohr *et al.*, 2000; Tréhu *et al.*, 2015).

A flexural trough and faulted terrace (Fig. 1) located outboard of the QCF are considered to be the hallmark geomorphic features of transpression here (Chase and Tiffin, 1972; Hyndman and Hamilton, 1993), yet these features are missing from the southernmost 80 km of the QCF. Instead, a low plateau 30–40 km wide lies outboard. The southern tip of the QCF is presently mapped as stepping over to the Revere–

Dellwood fault (RDF), which strikes southeast to the Explorer ridge (Davis and Riddihough, 1982; Carbotte *et al.*, 1989; Davis and Currie, 1993; Rohr and Furlong, 1995; Rohr and Tryon, 2010). The Tuzo Wilson seamounts (TWS) lie in an area of predicted extension in a right stepover on these right lateral offset faults.

In this article, recent changes in the tectonics of the southernmost QCF are proposed: propagation of the RDF into an overlapping and less transpressive configuration and a small reorientation of the QCF itself. Synthesizing seismicity data with bathymetry, gravity, sidescan, and seismic reflection data shows that the RDF extends ∼100 km farther north than previously thought. Along strike it becomes more parallel to the relative plate motion until it intersects the transpressionally deformed terrace and bends toward the QCF, becoming transtensional. It creates a distinct segment of the plate boundary that likely limited the southward rupture of the 2012 M_w 7.8 Haida Gwaii thrust earthquake. Inboard, the QCF has propagated southward into a slightly less transpressive orientation. The most transpressive segments of the plate boundary are being reoriented through fault propaga-
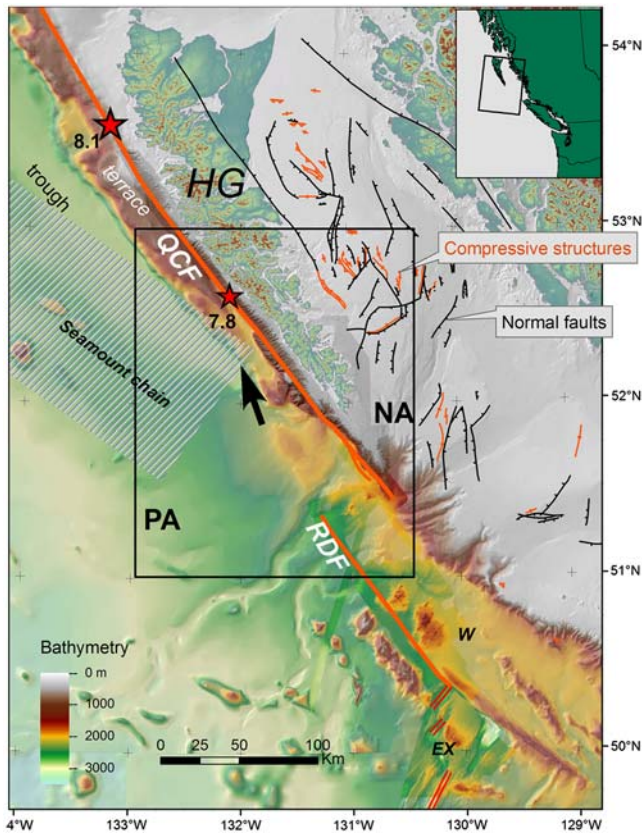
Figure 1. Bathymetry around Queen Charlotte fault (QCF) and Revere–Dellwood fault (RDF), draped over hill-shaded relief and illuminated from the northwest. Areas with multibeam bathymetry are darker. This is the traditional interpretation of the location of the QCF (Hyndman and Ellis, 1981). The forked southern tip of the QCF is based on sidescan data (Davis *et al.*, 1987b) and multichannel seismic reflection data (Rohr and Tryon, 2010). Structures on the continental shelf are Miocene extensional faults that have been compressed into positive flower structures during transpression on the QCF (after Rohr and Dietrich, 1992). EX, Explorer ridge; HG, Haida Gwaii archipelago; NA, North American plate; PA, Pacific plate; and W, Winona basin. Arrow indicates direction of relative plate motion using the midocean ridge velocity (MORVEL) model (DeMets *et al.*, 2010). The striped pattern indicates the approximate width of the Pacific plate affected by the Kodiak–Bowie seamount chain, as derived from a larger map. Black rectangle indicates area shown in Figure 2. Stars indicate the epicenters of the 1949 **M** 8.1 strike-slip earthquake and the 2012 M_w 7.8 thrust earthquake. Inset map shows extent of figure map in relation to Haida Gwaii. The color version of this figure is available only in the electronic edition.

tion. Large structures are discussed here; the many structural complications arising from the evolution of overlapping faults should be the subject of further study.

Tectonic History

The QCF off Haida Gwaii (Fig. 1) has been a strike-slip plate boundary between the Pacific and North American plates since ∼40 Ma (Hyndman and Hamilton, 1993). On average, it has been a pure strike-slip fault (Rohr and Currie, 1997), but in the last 5–6 Ma an ∼20° clockwise change in

relative plate motion (Atwater and Stock, 1998; Doubrovine and Tarduno, 2008) has resulted in transpression (Rohr and Currie, 1997). The midocean ridge velocity (MORVEL) plate motion model (DeMets *et al.*, 2010) results in 3° less rotation than the NUVEL-1A model (DeMets *et al.*, 1994) but with slightly greater speeds. The present relative plate motion at 52° N on the QCF is 50.2 ± 1 km/Ma and oriented 340 ± 2°, up to 20° more clockwise than the fault's strike. Transpression may be accommodated by subduction of the Pacific plate under the terrace (Hyndman and Ellis, 1983; Hyndman and Hamilton, 1993) and/or intraplate deformation (Horn *et al.*, 1984; Rohr *et al.*, 2000).

The southern terminus of the QCF is thought to have resided offshore northern Vancouver Island from 40 to 2 Ma (Davis and Riddihough, 1982; Wilson, 1988). After onset of transpression, it retreated 250 km northwest to its present position (Fig. 1), while offshore the RDF propagated to the northwest (Davis and Riddihough, 1982; Rohr and Tryon, 2010).

The TWS lie between the QCF and the RDF (Fig. 2); they have been interpreted to be a spreading center (Carbotte *et al.*, 1989), hotspot volcanism (Chase, 1977), or the result of extension in a right stepover between two right lateral strike-slip faults (Allan *et al.*, 1993). Geochemical studies were interpreted to indicate a near ridge but not a spreading-center origin for these seamounts (Cousens *et al.*, 1985). In multibeam data, the lack of pervasive extensional faulting argues for a lesser degree of extension (<100%) than in spreading centers and favors the stepover interpretation (Rohr and Furlong, 1995).

The Pacific plate adjacent to the QCF comprises chrons 3A–5, ∼6–10 Ma, with the anomalies trending nearly north–south (Wilson, 2002). Sediments on the plate are thought to be glaciomarine in origin and mostly deposited in the Pleistocene. The Kodiak–Bowie seamount chain trends southeast across the plate (Fig. 1); many seamounts are Miocene in age, but the Bowie seamount has also been volcanically active in the Holocene (Cousens *et al.*, 1985).

The North American plate east of the QCF consists of mafic Wrangellia terrane that was extended in the Miocene, probably with an element of strike-slip motion (Fig. 1) (Rohr and Dietrich, 1992). Extensional faults in the continental shelf have been transpressed into positive flower structures since the Pliocene (<5.3 Ma), at least one of which is seismically active (Rohr and Dietrich, 1992; Rohr *et al.*, 2000). How much transpression has been absorbed within Haida Gwaii is unknown (Rohr *et al.*, 2000; Smith *et al.*, 2003).

Data

Bathymetry, seismicity, sidescan data, gravity, and vintage seismic reflection profiles were interpreted and integrated for an interpretation of regional fault locations and crustal deformation. They provide a picture of large-scale patterns of deformation; creating a detailed map of structures between the faults would require new data. Three additional decades of earthquake documentation since the presently accepted
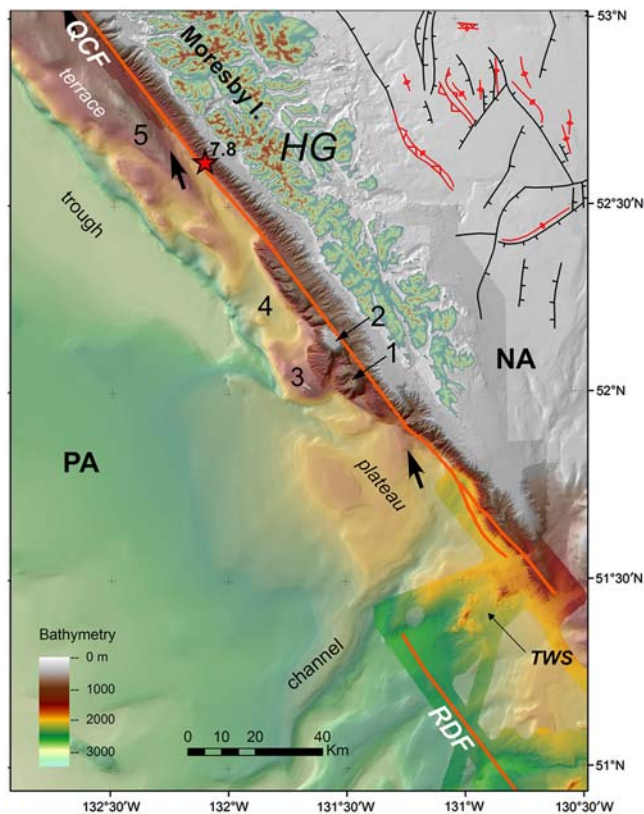
Figure 2. Bathymetry around southern QCF and northern RDF, draped over hill-shaded relief and illuminated from the northwest. Areas with multibeam bathymetry are darker. The Tuzo Wilson seamounts (TWS) formed in the right stepover between these two right lateral strike-slip faults. Morphologic features: (1) and (2) bathymetric highs west of the QCF, (3) southernmost portion of the terrace, (4) a depressed area of the terrace, and (5) ridge parallel to the QCF. Arrows indicate direction of relative plate motion using the MORVEL model (DeMets *et al.*, 2010); the predicted degree of transpression is greater in the south than the north as the strike of the QCF changes. The morphology of the terrace and trough are not present over the southernmost section of the QCF; instead, a broad plateau is rimmed by a small sedimentary fan. Abbreviated labels are as in Figure 1. Stars indicate the epicenters of the 1949 **M** 8.1 strike-slip earthquake and the 2012 M_w 7.8 thrust earthquake. The color version of this figure is available only in the electronic edition.

tectonic framework off the west coast of Canada was published (Hyndman *et al.*, 1982) prompted a reinterpretation of vintage seismic reflection and sidescan data.

Geomorphology

Bathymetry (Figs. 1 and 2) outboard of the QCF is generally characterized by topography that strikes parallel to slightly oblique to the fault. The map shown here has been collated from traditional echo sounding (Canadian Hydrographic Service, 1983), and multibeam surveys of the TWS (Rohr and Furlong, 1995) and the QCF (Barrie *et al.*, 2013). These multibeam surveys have horizontal resolution of 30 and 5 m, respectively.

Offshore Moresby Island of Haida Gwaii, the QCF has traditionally been thought to be oriented subparallel to the

shelf break and to be located at the foot of the adjacent slope (Fig. 2). Between 52° N and 52°25′ N, a series of highs cut by east–west valleys lie just west of the fault. The highest one (labeled 2 in Fig. 2) has been interpreted to be a translated piece of continental shelf, and the high to its south (1 in Fig. 2) has been interpreted to be a volcano (Barrie *et al.*, 2013). Farther south, sidescan sonar shows that the tip of the QCF forks (Davis *et al.*, 1987b) and multichannel seismic reflection data (Rohr and Tryon, 2010) east of the TWS imaged the fault, cutting through sediments that have different stratigraphic patterns on either side.

The RDF around 51° N has tens of meters of relief (Rohr and Furlong, 1995) and forms a lineation in sidescan data (Davis *et al.*, 1987b; Carbotte *et al.*, 1989; Davis and Currie, 1993). Immediately north of the TWS, however, no lineation on the seafloor was recognized in the sidescan data by Carbotte *et al.* (1989).

West of the QCF, features on the seafloor (Fig. 2) comprise the TWS, a sedimentary channel, a plateau at depths of 1850–1950 m, and the Queen Charlotte terrace at depths of 800–1000 m. The terrace is characterized by faulted and folded sediments that form ridges subparallel to the continental shelf break (Chase and Tiffin, 1972; Hyndman *et al.*, 1982). The southernmost part of the terrace is broken up into a block (labeled 3 in Fig. 2), a depressed area (4 in Fig. 2), small west-northwest-to-northwest-trending ridges and a large ridge that flanks the west side of the QCF (5 in Fig. 2). The southwestern corner of the terrace (∼1600 m deep) is capped by a narrow peak of unknown origin that rises to 1000 m. The southern block's western edge is defined by a ridge that is subparallel to the direction of the Pacific–North American relative plate motion.

West of the plateau, seafloor depths (Fig. 2) increase gradually in what appears to be a sedimentary fan. At 52° N, the Queen Charlotte Trough begins suddenly as a narrow, steep-sided depression. It widens along trend to the northwest and lies at about 2900 m depth.

The continental slope rises steeply to a 5 km wide continental shelf and the peaks of Moresby Island (Fig. 2). These peaks have an average height of 550–600 m in the south, rising to 850–900 m around 52°30′. The Haida Gwaii archipelago widens along its northwesterly trend.

Seismicity

A map of moment tensor solutions (Fig. 3) (Kao *et al.*, 2012) shows that seismicity extends 65 km north of the traditional limit of the RDF, implying that this fault is active over a greater distance than previously inferred. Solutions are from January 1995 to September 2012 and range from M_w 3.9 to 6.4. Braunmiller and Nabelek (2002) noted the occurrence of earthquakes up to 20 km north of the mapped tip of the RDF but did not map an extension to the RDF. Locations in this area are known to be biased by the shore-based seismographs and use of a regional continental velocity function (Berubé *et al.*, 1989; Bird, 1997; Ristau *et al.*, 2007), but locations of these
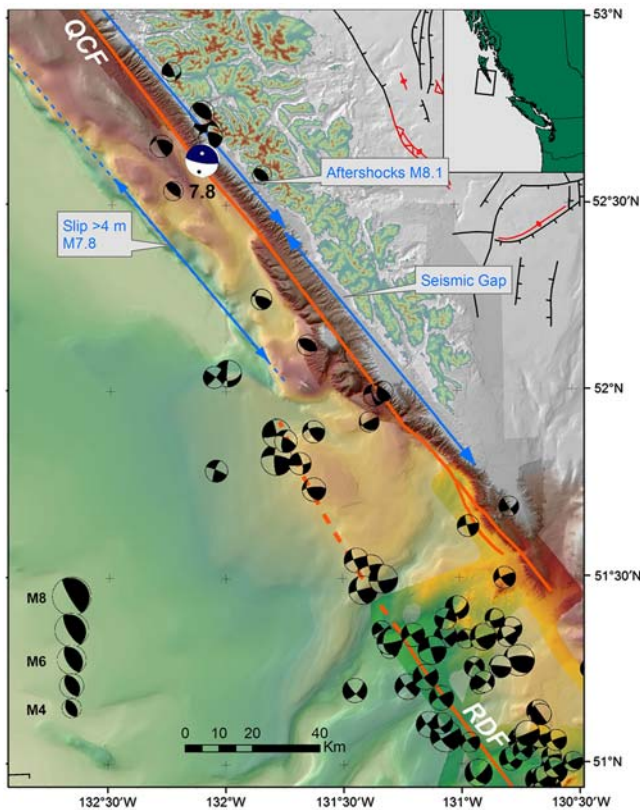
Figure 3. Central moment tensor solutions from January 1995 to September 2012 (Ristau *et al.*, 2007; Kao *et al.*, 2012). The moment tensor solution for the 2012 M_w 7.8 earthquake is from Kao *et al.* (2015). A number of strike-slip earthquakes have occurred along a projected trend of the RDF (dashed line). The extent of rupture of the 1949 **M** 8.1 strike-slip earthquake (Bostwick, 1984; Rogers, 1986) and inferred seismic gap (Rogers, 1986) are shown as arrows. Lateral extant of rupture greater than 4 m of the 2012 M_w 7.8 earthquake (Nykolaishen *et al.*, 2015) is shown as an arrow on the west side of the terrace. The dashed line indicates rupture less than 4 m, but typically ∼2 m. Inset map shows extent of figure map in relation to Haida Gwaii. The color version of this figure is available only in the electronic edition.

larger events are considered reliable to 10 km. An M_w 6.4 event occurred at the northern end of the inferred fault 35 km west of the QCF. Records of this event were closely examined to confirm that it had occurred well offshore (J. Cassidy, personal comm., 2009). Interpreted depths of the events range from 6 to 18 km but are poorly constrained.

Along this newly recognized fault, focal mechanisms are dominantly strike slip, with some obliquely compressive events (Fig. 3). Seventy five percent of the fault planes dip at angles greater than 60°. Transpressive events of **M** 4 occur within 10 km of the QCF, coincident with folds of the terrace. Numerous events occurred between the southern tip of the QCF and the RDF (Braunmiller and Nabelek, 2002; Ristau *et al.*, 2007); many of their slip vectors are nearly parallel with the relative plate motion vector (Rohr and Tryon, 2010).

The southernmost point of rupture from the 1949 **M** 8.1 strike-slip earthquake on the QCF (Fig. 3) was ∼52°25′N

(Bostwick, 1984; Rogers, 1986) and was defined by aftershocks with **M** > 4.5. To the south a seismic gap is thought to exist; it was first noticed by Sykes (1971) and further described by Rogers (1986) and Berubé *et al.* (1989). An **M** 7 event occurred near the southern tip of the QCF in 1970; the only large earthquake to occur in this section of the plate boundary has been the 2009 M_w 6.4 on the RDF.

Aftershocks of the 2012 M_w 7.8 earthquake occurred predominantly north of 52°15′ and have been interpreted as indicating the along-strike extent of the rupture surface of this earthquake (Fig. 3) (Farahbod and Kao, 2015; Kao *et al.*, 2015; T. Mulder *et al.*, unpublished manuscript, 2015). They are coincident with the southern section of the plate boundary ruptured by the 1949 **M** 8.1 earthquake. The QCF within the seismic gap did not rupture, and there was comparatively little activity offshore in the region of the RDF–QCF overlap, implying that this part of the plate boundary is a distinct segment. An estimate of rupture from the 2012 M_w 7.8 earthquake was calculated with heavy smoothing from Global Positioning System (GPS) observations (Nykolaishen *et al.*, 2015) and the model of Lay *et al.* (2013); it shows that rupture was concentrated west and southwest of the epicenter (Fig. 3).

Sidescan Sonar

In the sidescan data (Fig. 4), three main features relevant for this study are a patch of high backscatter interpreted as basalt flows (Carbotte *et al.*, 1989), a scarp that strikes north across the terrace, and a lineation on the seafloor at ∼52°30′N (Davis *et al.*, 1987a). SeaMARC II sidescan mosaics (see Data and Resources) were scanned, georeferenced, and interpreted. The instrument's ∼10 km swath has horizontal resolution of 5 m. Data surrounding the TWS have been interpreted (Carbotte *et al.*, 1989), but data further north have not been previously interpreted.

Northwest of the TWS, basalt flows ∼7 km across in map view (Fig. 4) and less than 10 m thick were interpreted (Carbotte *et al.*, 1989) to lie on top of the sediments. This very bright patch of backscatter sits at the southern end of a longer area of bright backscatter, which could be generated from coarse clastic sediments in sedimentary channels and/or thinly sedimented basalt flows. Several circular features less than a kilometer in diameter can be seen in the flows (Davis *et al.*, 1987b), suggesting the existence of small volcanic cones.

An 18 km long fault scarp trends north across the northwest-trending terrace (Fig. 4); it is interpreted here to be the northernmost extent of the RDF. The scarp can be connected to the RDF interpreted from seismicity (Fig. 3) by the ridge that is subparallel to plate motions. No further surface expression of the fault can be seen in the sidescan data, and the multibeam systems were not able to map at these water depths. These data cannot be used to determine whether the RDF joins the QCF at depth. Regardless, the right stepover between two right lateral strike-slip faults results in local transtension, which disrupts the terrace and creates the morphologic depression seen here.
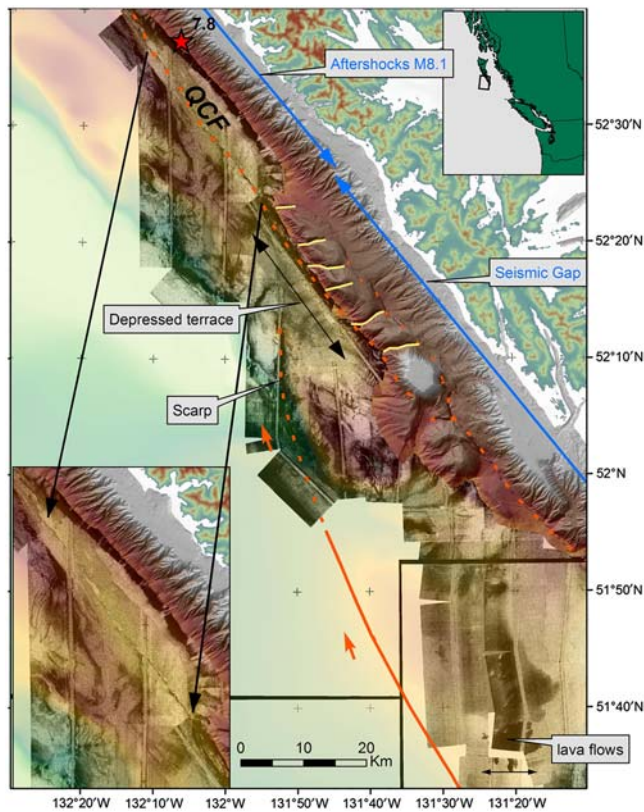
Figure 4. Mosaic of SeaMARC II sidescan sonar data (Davis *et al.*, 1987a, b). High values of backscatter are shown in black. A transparent layer of bathymetry (as in Fig. 1) lies on top. Dashed lines indicate fault positions interpreted from both sidescan and multibeam data. The solid line is the extension of the RDF inferred from seismicity (Fig. 3). Short arrows are parallel to the relative plate motions. The inset map (lower left) shows a trace of the QCF in the sidescan data; it connects to the west of the small highs, not the east as in the traditional interpretation of the QCF (Fig. 1). This results in a compressive left step with respect to the southernmost section of the fault near 52°5′ N. A ridge at ∼52° N, 131°40′ W is oriented subparallel to the plate motions. A scarp cuts across the terrace in a northerly direction. These features are interpreted here to be formed by northward propagation of the RDF. An ∼7 km black lobate backscatter anomaly in the lower right portion of the map has been interpreted to be seafloor lava flows (Carbotte *et al.*, 1989). Inset map shows extent of figure map in relation to Haida Gwaii. Stars indicate the epicenters of the 1949 **M** 8.1 strike-slip earthquake and the 2012 M_{w} 7.8 thrust earthquake. The color version of this figure is available only in the electronic edition.

A lineation that strikes over 30 km (inset Fig. 4) to the western edge of the series of bathymetric highs is interpreted to be the QCF; this differs from the previous interpretation (Fig. 1), which placed the fault east of the highs (Hyndman and Ellis, 1981). Its trace connects to a scarp on the western side of the highs and is again clearly seen southeast of the shallowest high. This interpretation describes a compressive left step in the QCF. The highs become more clearly defined and shallow from 1400 to 750 m toward the stepover, with the shallowest one reaching 240 m depth. Because it is adjacent to a compressive left step, it is interpreted here to be a pop-up structure rather than a translated fragment of continental shelf
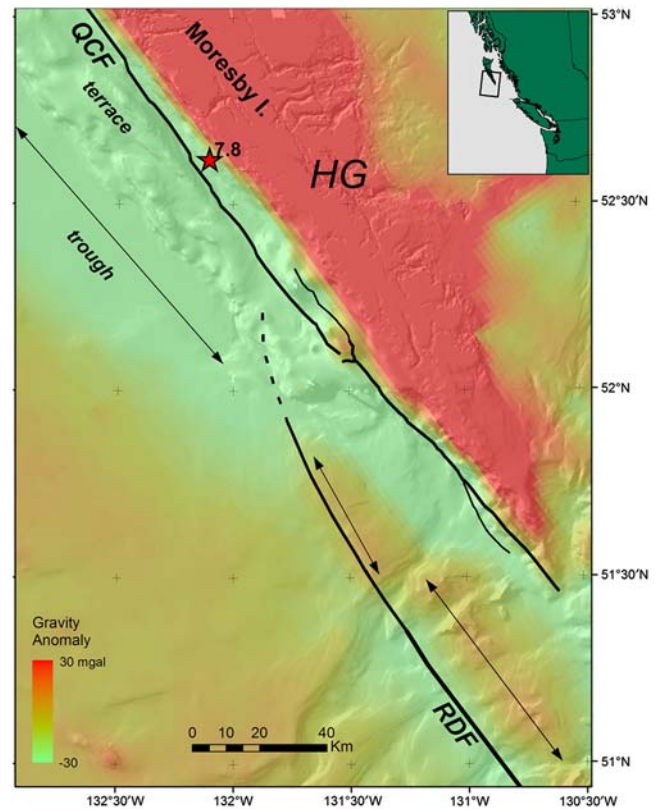

Figure 5. Gravity anomaly shown as a transparent layer above shaded bathymetric relief; free air anomaly is displayed at sea and a Bouguer anomaly over land. Locations of QCF and RDF are shown as interpreted from seismicity (Fig. 3) and sidescan data (Fig. 4). A 30 mGal low corresponds to the trough, but small amplitude elongate highs to the southeast are subparallel to the RDF. Inset map shows extent of figure map in relation to Haida Gwaii. Stars indicate the epicenters of the 1949 **M** 8.1 strike-slip earthquake and the 2012 M_{w} 7.8 thrust earthquake. The color version of this figure is available only in the electronic edition.

(Barrie *et al.*, 2013). Incised valleys strike east-northeast across the highs and are interpreted to be faults. An incised valley is located to the east of the hills and is interpreted to be the eastern branch of the QCF that dies out to the northwest. In this new interpretation, the QCF has propagated south in a series of left steps; the east-to-east-northeast-striking faults are compressive and have uplifted small pop-up structures that have been successively abandoned. The QCF here is now 5° less transpressive in its orientation to relative plate motion vectors than previously interpreted.

Gravity Anomaly

The free air gravity anomaly map (Fig. 5) most strikingly shows high values over Moresby Island and low values along the trough and terrace (Horn *et al.*, 1984; Dehler and Clowes, 1988). Low values along the trough terminate just south of 52° N, indicating that the morphologic expression of the trough is the real limit of the Pacific plate's flexural response to transpressive loading and is not simply indicative of a trough filled with sediments south of 52° N. A low-
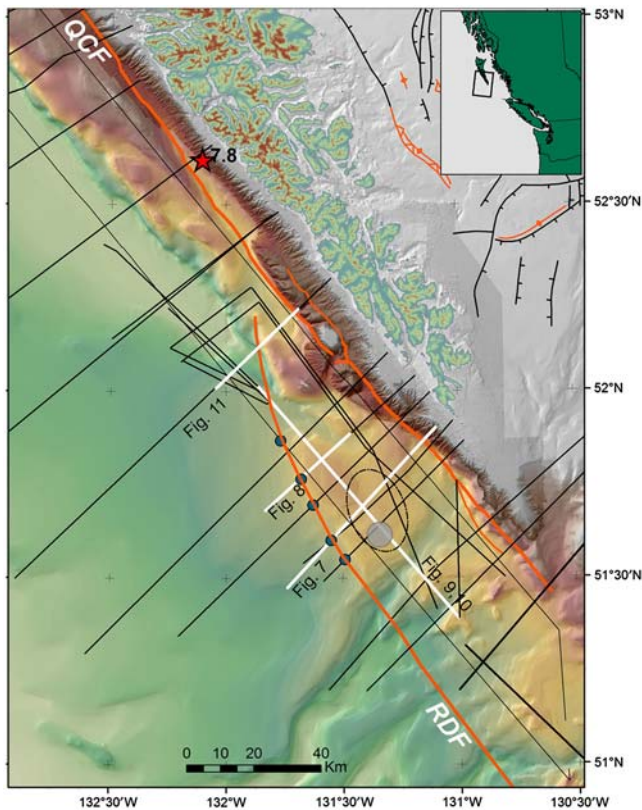
Figure 6. Locations of vintage singe channel seismic reflection profiles, many of which are in Davis and Seeman (1981). Bold white lines mark the reflection sections shown in Figures 7–11. The large light gray circle is the approximate area of seafloor lava flows (Fig. 4). The ellipse shows the approximate area of diffractions in seismic sections interpreted to be flows and intrusions throughout the sediments. Small dark gray filled circles show areas of basement deformation and uplift observed in seismic reflection lines. The trace of the RDF has been adjusted a few kilometers to the west of the location inferred from seismicity (Fig. 3). Inset map shows extent of figure map in relation to Haida Gwaii. Star indicates epicenter of 2012 M_w 7.8 earthquake. The color version of this figure is available only in the electronic edition.

amplitude local high trends northwest under the plateau and is offset ∼10 km in a left lateral sense under the sedimentary channel. South of 52°5′, the QCF is nearly coincident with the steep gradient in values associated with the continental shelf break, but the left step to the north has changed the strike 5° clockwise, away from the shelf break trend and closer to the direction of the relative plate motions.

Seismic Reflection Profiles

Analog single-channel seismic reflection profiles (Fig. 6) imaged faulted oceanic crust under the inferred trace of the RDF, numerous diffractions under the basalt flows, and inactive folds under the depressed terrace (labeled 4 in Fig. 2). Profiles were collected west of the QCF between 1967 and 1994. These unmigrated shallow sections have limited ability to detect structures in steep topography; they tend to be overwhelmed by diffractions. Line drawings of five profiles were

presented by Chase and Tiffin (1972), four of which have been subsequently presented (Hyndman *et al.*, 1982). Uninterpreted sections are available in an open file (Davis and Seeman, 1981). In addition, two lines parallel to regional trends were collected by the U.S. Geological Survey (USGS; Bruns *et al.*, 1992; Walton *et al.*, 2015), and four lines across or near the TWS were presented by Carbotte *et al.* (1989). Air-gun sources ranged from 5 to 160 in³; the quality of the recordings varies significantly. Most work has stressed the steep and rugged topography of the terrace.

Line 78-12660 crossed the plateau (Fig. 7) into the Pacific plate and imaged two fault zones: one under the plateau edge with a net vertical separation of ∼500 ms two-way time (500 m, assuming an acoustic velocity of 2 km/s in the sediments) and another fault ∼15 km to the southwest, also with a net vertical separation of ∼500 m. The fault to the southwest deforms the oldest sediments and is not associated with a bathymetric feature. About 10 km to the north, several ∼100 m steps in basement are in a similar position 15–20 km west of the plateau. Sediments in the plateau have been progressively tipped down to the northeast. Angular unconformities in the shallowest sediments indicate that tilting continues to recent times and that these are growth strata. The dip of the basement faults cannot be determined, but the uplift is significant. Carbotte *et al.* (1989) showed a portion of line 78-12660 that covers the eastern fault under the plateau edge and interpreted it as an inactive portion of the RDF. However, the ongoing tilt of the uppermost sediments and the correlation of recent seismicity with the plateau edge (Fig. 7) indicate that this fault is, in fact, active. Within a few kilometers of the QCF, sediments have been tipped up slightly (Fig. 7). To the north, folds and faults occur over a wider area and increase in amplitude as the terrace is approached.

Line 78-12660 crossed the plateau about 5 km north of the lava flows. A few bright spots occur in the sediments above a region with diffuse-to-absent reflectivity; however, southwest of the bright spot, layering can be observed down to 3.5 s. Because of the proximity to lava, the bright spots and lack of reflectivity are interpreted to be more lava flows and/or irregular intrusive features in the sediments. These features have not been previously interpreted.

Line 72-10 (Fig. 8) imaged uplift of oceanic basement of 300 ms two-way time (300 m, assuming an acoustic velocity of 2 km/s) on the inferred RDF and another 300 ms within 5 km northeast of this fault. Traces were not recorded long enough to image oceanic crust southwest of the RDF. Several near-vertical faults cut sediments within or close to the zone of recent earthquakes. One fault comes within 250 ms of the seafloor but cannot be traced to the reflection line to the south, and the line to the north has a low signal-to-noise ratio.

Basement uplift of up to 600 ms two-way time (600 m, assuming an acoustic velocity of 2 km/s) is observed under the western edge of the plateau on three other reflection lines. Deformation occurs over a width of several kilometers, for example, 5 km on line 78-12660 (Fig. 7). New strike-slip faults often consist of multiple strands that coalesce over
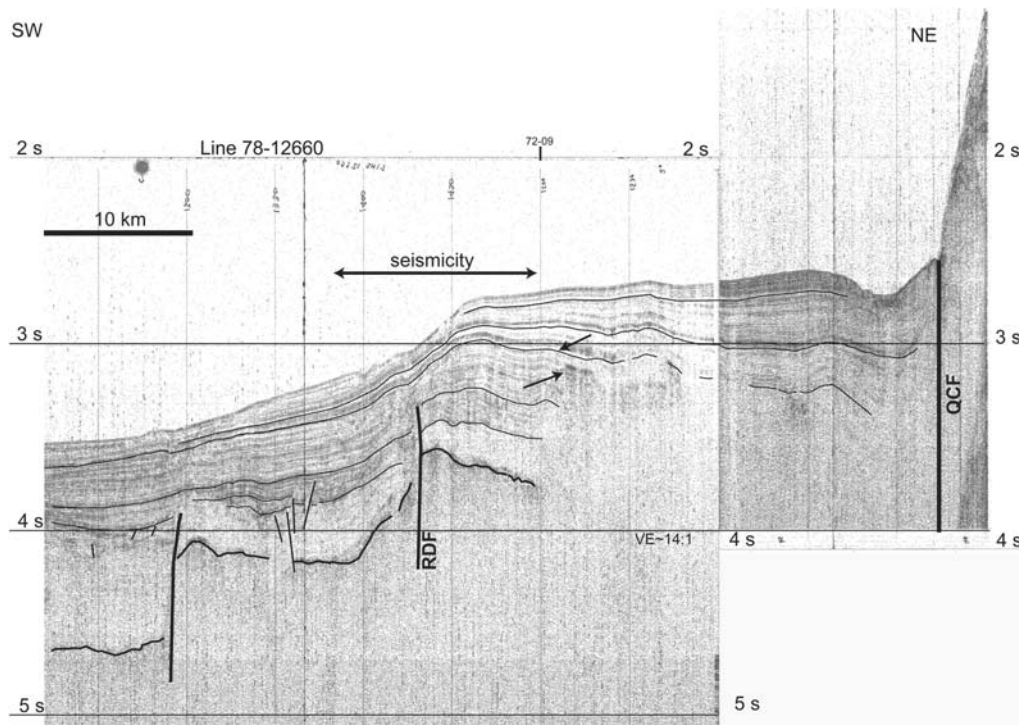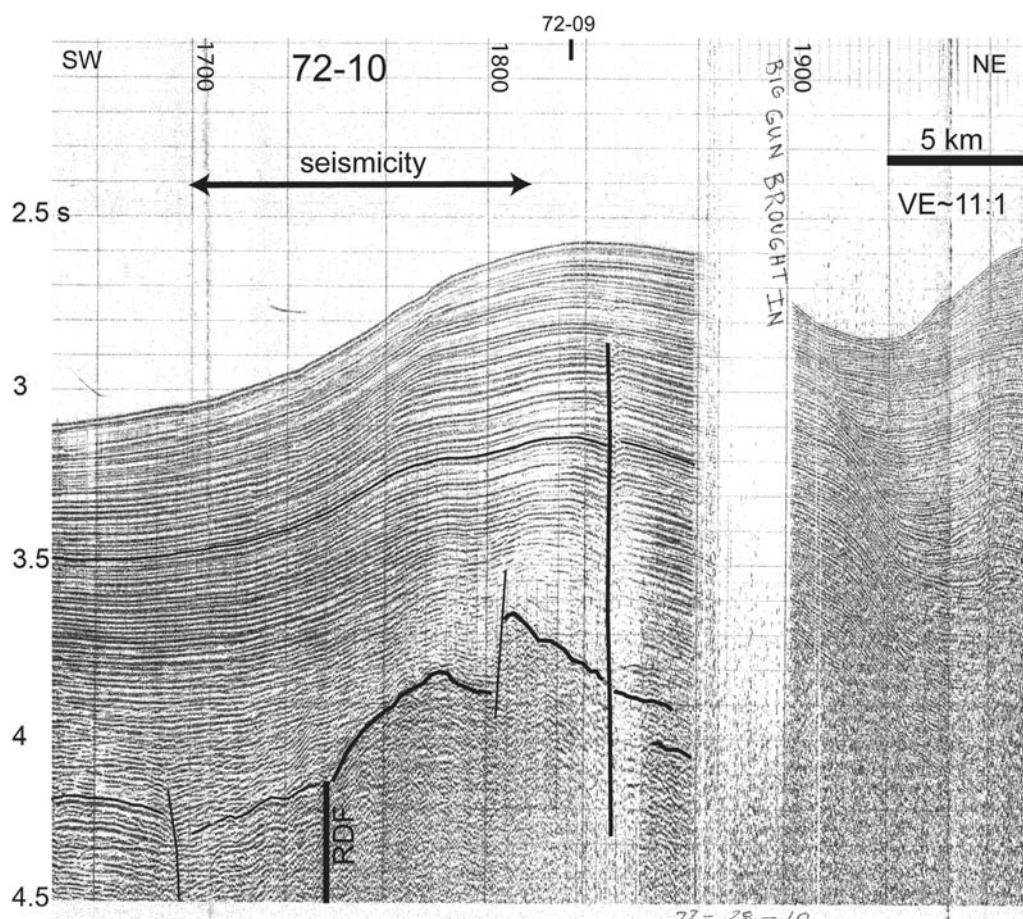
Figure 7. Single-channel seismic reflection line 78-12660 collected in 1978 using a 20 in³ air gun (Davis and Seeman, 1981). The vertical axis is two-way travel time. Vertical exaggeration (VE) is ∼14 : 1. Seismicity correlates with a 500 ms net vertical separation in oceanic crust (thicker line) and is interpreted to be part of the RDF. A second fault of equal vertical separation occurs 15 km to the southwest but is not associated with seafloor topography. Ongoing tilting of sedimentary layers between the RDF and QCF indicates recent tectonic activity in this block. The downward pointing arrow indicates an angular unconformity and the upward pointing arrow indicates a brightened reflector. Note the abrupt termination of sedimentary reflectors to the southwest and the lack of reflectors beneath the bright reflector and to the northeast along the line. The location is given in Figure 6.

time (Wilcox *et al.*, 1973), and transpression can create positive flower structures in which faults fan out as they shallow. The maximum uplift of oceanic crust correlates with strike-slip seismicity (Fig. 3). Surficial deformation lies in the western side of the zone of earthquakes (Fig. 6) and the location of the inferred RDF was refined and shifted two kilometers to the west. A single fault is drawn in Figure 6 to emphasize the big picture and because current data do not allow structures to be mapped in detail.

Line 72-09 imaged a number of near-vertical faults with small vertical separation and diffractions in the sediments (Fig. 9). The line ran along strike of the plateau and crossed the lava flows. Faulting cuts the seafloor north of the flow and continues to the north, penetrating 600–1000 ms into the sedimentary section. A 40 m step in bathymetry (Fig. 2) corresponds to the fault at 1035 (Fig. 9). The fault strikes east-northeast, as predicted for conjugate shear assuming a simple strain model for northwest-directed right lateral strike-slip deformation. A number of near-vertical faults are also observed on a seismic line that runs parallel to regional strike on the outer edge of the plateau (USGS line F-7-89-EG-58; see Data and Resources). The fact that many faults were imaged in an along-strike profile and few across strike within the plateau profile suggests that the faults strike at a high angle to the RDF, likely as conjugate strike-slip faults.

Although not all faults imaged by line 72-09 reach to the seafloor, faulting is likely recent. North of the lava flows, the line lies within the zone of seismicity shown in Figure 3. Strike-slip faults do not necessarily create vertical separation of reflectors and can go undetected in seismic sections. In addition, deformation in the northern plateau is likely younger and has less net displacement than in the southern plateau. On the Nootka fault between the Explorer and Juan de Fuca plates, thin sediments were faulted to the seafloor (Hyndman *et al.*, 1979). Adjacent to the continental margin, however, where sediments are greater than 1 s thick, faults do not propagate to the seafloor (M. Riedel, personal comm., 2014), although **M** > 5 earthquakes are often recorded there (Earthquakes Canada, 2014; see Data and Resources).

Line 72-09 crossed the basalt flows (Fig. 10) imaged in the sidescan backscatter data (Fig. 4). Diffractions above the seafloor in the seismic reflection data were probably generated by small volcanic cones here inferred to exist from circular features in the sidescan data (Davis *et al.*, 1987b). The seafloor itself consists of overlapping short diffractions, as would be generated by basalt. In the sediments, a broad group of diffractions shallows toward the flow (see also Fig. 9). They were probably generated from irregular basalt flows and intrusions in the sediments. Disrupted sedimentary reflectors, bright spots, and diffractions are visible

Figure 8. Single channel seismic reflection line 72-09 collected in 1972 using a 120 and a 40 in³ air gun from 1630–1840 and a 40 in³ air gun after 1900. Although the data were not recorded long enough to image oceanic crust to the southwest, fault-bounded uplifted basement of the plateau can be seen. The fault lies within the zone of seismicity (Fig. 3) and is interpreted to be part of the RDF. Vertical axis is two-way travel time; VE is ~11 : 1. The location is shown in Figure 6.
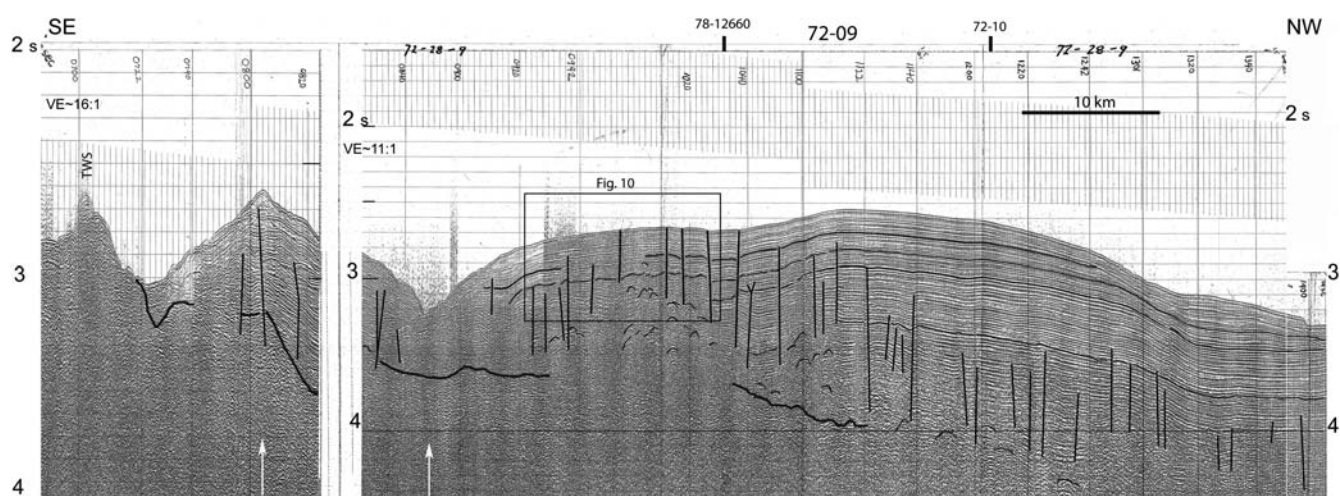
Figure 9. Single channel seismic reflection line 72-09 collected in 1972 using a 120 and a 40 in³ air gun. In the southeast, the TWS are visible as rough highly reflective seafloor. Sediment thickness increases abruptly over a faulted and tilted crustal block between white arrows. To the northwest, many near-vertical faults can be observed cutting the sediments and disturbing the seafloor (e.g., at 1020). A group of diffractions shallow toward the crossing of the lava flows seen in the sidescan data (Fig. 4). The vertical axis is two-way travel time; VE is 11:1. The location is shown in Figure 6.
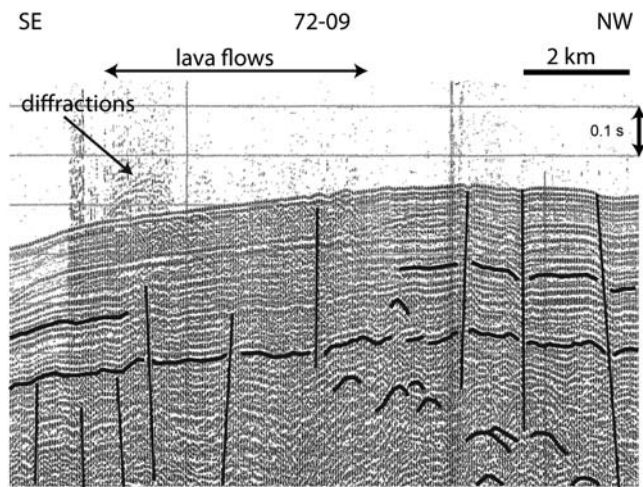
Figure 10. Detail from reflection line 72-09 (Fig. 9) shows diffracting character of lava flows on the seafloor. Diffractions above the seafloor are probably from small cones nearby that were imaged as small circular features in sidescan data (Davis *et al.*, 1987b). In the sediments, diffractions could be from irregular igneous flows or intrusions. The vertical axis is two-way travel time; VE is ~11 : 1.

on five adjacent seismic profiles, defining an ~20 × 30 km area of inferred igneous activity (Fig. 6). Small isolated bright spots can be observed in seismic reflection data over the plateau outside this area.

The onset of volcanism is unknown but may have begun in the Pleistocene after deposition of a significant thickness of sediments. Otherwise a single coherent igneous edifice would be visible with sediments onlapping its sides. The lava flows on the seafloor indicate very recent activity, possibly less than 10 Ka, which is the approximate age of the termination of the last major influx of glacial sediments.

Across the depressed portion of the terrace (4 in Fig. 2), line 78-12415 (Fig. 11) shows seafloor-parallel reflectors that have filled in over deeper folded sediments, suggesting that a once transpressional environment is now experiencing subsidence. This is a marked contrast to reflection profiles immediately to the north (Chase and Tiffin, 1972; Hyndman *et al.*, 1982) that show ongoing folding.

Synthesis and Discussion

Close examination of a variety of datasets shows that the plate boundary is being reoriented by southward propagation of the principal displacement zone of the QCF and by northward propagation of an offshore fault, the RDF (Fig. 12). Both changes result in a less transpressive orientation of the plate boundary. Segmentation of the plate boundary interpreted here is coincident with the southern limits of rupture in both the 1949 **M** 8.1 (Bostwick, 1984; Rogers, 1986) and the 2012 M_{w} 7.8 (James *et al.*, 2013; Lay *et al.*, 2013; Farahbod and Kao, 2015) events.

The QCF now trends 5° differently than the steep continental slope between 52°5′ and 52°40′, as is clearly seen in the gravity data (Fig. 5). The shelf break and slope are
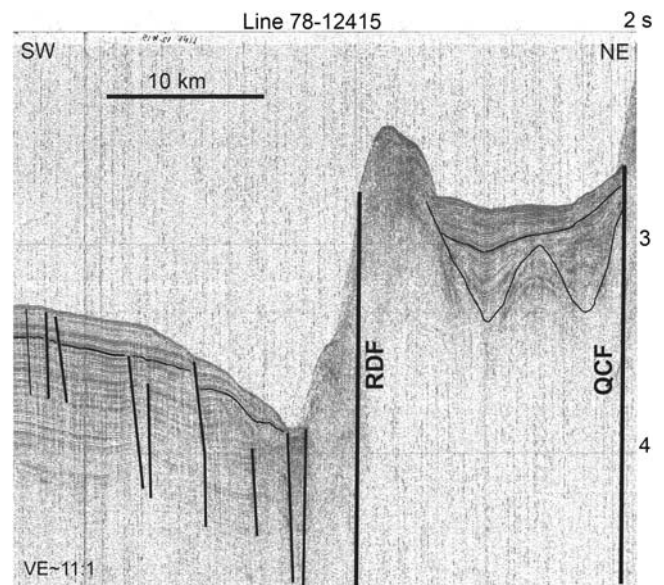

Figure 11. Single channel seismic reflection line 78-12415 crosses the depressed area of terrace (number 4, Fig. 2), where deeper folds are overlain by gently dipping layers. The interpreted northern section of the RDF defines the steep scarp. The beginning of the Queen Charlotte Trough is evident in the narrow steep-sided depression and faulted sediments. Vertical axis is two-way travel time; VE is ~11 : 1. Location shown in Figure 6.

subparallel to relative plate motions from ~40 to 6 Ma. The present orientation is, however, 5° closer to present day relative plate motions, but still at a transpressive angle of ~15°. The QCF appears to have propagated southward in a series of left steps relative to the fault segment to the south creating a series of pop-up structures. Multibeam and sidescan sonar data show the surficial trace of deformation. It would not be possible to determine whether the deeper fault zone has also been reoriented until earthquake locations have horizontal errors of, at most, 2 km. Three microseisms were located by an ocean-bottom seismometer (OBS) array (Hyndman and Ellis, 1981) 18–21 km deep under the southeast side of the highest high (~52°7′N; 2 in Fig. 2), suggesting that at least some deep deformation is still occurring on the east branch of the QCF.

Seismicity, faulting, and tilting of oceanic crust and igneous activity collectively indicate that the RDF is active 100 km farther north than previously thought (Fig. 12). First, an inferred fault was drawn through earthquakes that trended north of the known RDF. The fault's location coincides with the western edge of a small plateau and, by extension, a ridge in the terrace farther north. Seismic reflection data image 500–600 m of uplift of oceanic crust under the edge of the plateau, and sidescan data image a fault scarp that cuts across the terrace. Gravity data confirm that features seen in bathymetry and seismic reflection data are in fact expressive of plate deformation and show the areal extent of segmentation of the Pacific–North American plate boundary.

Although each dataset considered has its own inaccuracies in location or navigation, the coincidence of features
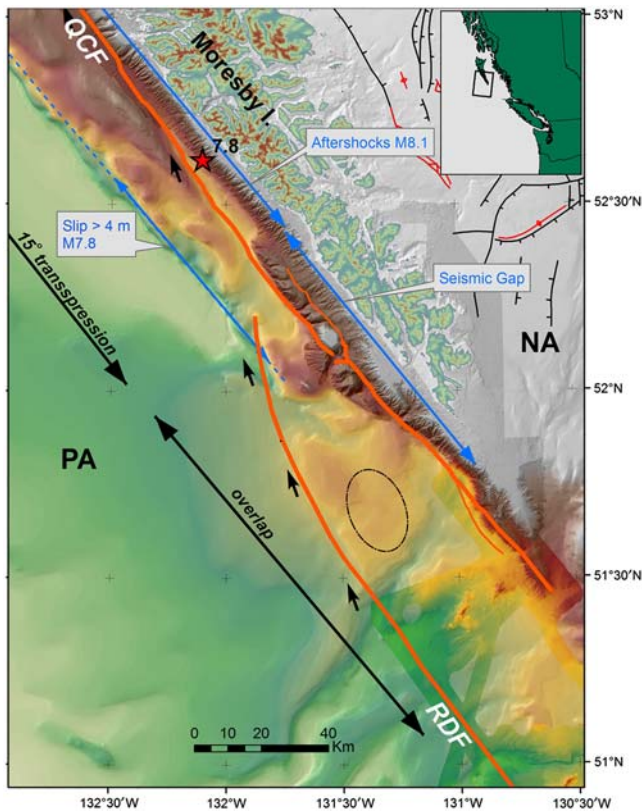
Figure 12. Northward propagation of the RDF. Location of the RDF as interpreted here from seismicity, sidescan, gravity, and seismic reflection data. Segments of the plate boundary are indicated: one comprising overlap between the QCF and the RDF and one that is in 15° transpression. The latter is the segment that ruptured in the 2012 M_w 7.8 thrust earthquake. Lateral extent of this earthquake's rupture greater than 4 m (Nykolaishen *et al.*, 2015) is shown as an arrow on the west side of the terrace, whereas the dashed line indicates rupture less than 4 m but typically ~2 m. Black arrows indicate relative plate motions on the RDF. Compression across the RDF at 51° 30′ is 7 km/Ma less than that predicted for the QCF at the same latitudes at the full rate of relative plate motions, 17 km/Ma. The ellipse shows the newly interpreted region of igneous activity between the faults. Predicted transtension between the two faults is also evident in the depressed section of the Queen Charlotte terrace that the fault transects. On Moresby Island, peaks inboard of the overlap segment are several hundred meters lower than inboard of the 15° transpressive segment of plate boundary to the north. Stars indicate the epicenters of the 1949 **M** 8.1 strike-slip earthquake and the 2012 M_w 7.8 thrust earthquake. The color version of this figure is available only in the electronic edition.

lends confidence that the RDF is active well north of its traditionally located termination. New data, with modern navigation, would no doubt define the location of activity better. The RDF as drawn in Figure 12 is a generalized location; strike-slip faults often consist of several strands, can be complicated by conjugate faulting, and may end in splays (e.g., Wilcox *et al.* 1973; Kim *et al.*, 2004).

Seismicity on the northern extension of the RDF is characterized by strike-slip faulting with some oblique compressive focal mechanisms. The predicted angle of transpression along the RDF decreases from 15° to 0° between 51°30′ and

52° N. If the RDF were carrying the full Pacific–North American relative motion, the rate of convergence would start at 10.5 km/Ma and decrease to 0° between 51°30′ and 52° N, but the actual rate is less than this because the southernmost QCF is still active.

Seismic reflection data have imaged up to 500–600 m uplift on the RDF, but the single channel data cannot resolve the attitude of faults at depth. They appear steep, which is congruent with the strike-slip focal mechanisms and overall transpressive stress. This is in contrast to a purely compressional deformation front, such as northern Cascadia, where thrust faults are spaced 5–10 km apart, flatten near the seafloor, and do not cut basement (Hyndman *et al.*, 1994; Shaw *et al.*, 2005).

Propagation of the RDF within the Pacific plate has broadened the Pacific–North American plate boundary, because motion between the two plates is shared over a 10–40 km width between these two main faults. The RDF is oriented closer to the direction of the relative plate motion than the QCF at these latitudes, but there is still a transpressive component to the relative motion across the fault. The RDF could be seen as contributing to an evolution toward a principal displacement zone parallel to relative plate motions. Initiation and propagation of the RDF along the Winona basin to the TWS is thought to have occurred since 2 Ma, while the QCF retreated ~250 km to the northwest (Davis and Riddihough, 1982; Rohr and Tryon, 2010). Local propagation of the QCF at ~52.2° N has reoriented the fault by ~5° but does not change its overall length. (A 7 km step-over does not seem to warrant renaming the southernmost segment of the QCF.) Farther south, on the Pacific–North American plate boundary, propagation has been an important process in the evolution of the San Andreas fault system (e.g., Wakabayashi *et al.*, 2004). If the plate boundary here evolves toward a more efficient configuration, the RDF fault might assume most, if not all, of the relative plate motions, effectively bypassing the southern QCF and transferring oceanic crust presently between the RDF and the QCF to the North American plate.

Overlap

Northward propagation of the RDF results in overlap of 120 km with the QCF. A right step in a right lateral strike-slip fault system predicts that northwest-directed transtension would occur, but stresses can be complex and vary locally (Mann, 2007). To investigate this process in the overlap area only, surficial mapping and a few shallow penetrating vintage seismic reflection profiles of the subsurface are available.

Extensional stresses are evident at the southern end of the fault overlap in the TWS (Allan *et al.*, 1993; Rohr and Furlong, 1995) and likely at the northern end in the depressed area of the terrace. This mapping confirms previous interpretations that the TWS are the result of fault overlap (Allan *et al.*, 1993; Rohr and Furlong, 1995) and are not a spreading center creating oceanic crust. Igneous activity

is also observed 25–50 km north of the TWS as surficial lava flows and an irregular igneous complex in the sediments (Figs. 3 and 10). The igneous activity may have initiated after the tip of the RDF had migrated past. Extension of the young oceanic plate could easily release partial melt in the astheno-sphere, which is no more than a few tens of kilometers below basement. In addition, this patch of volcanism is on the trend of the Kodiak–Bowie seamount chain (Fig. 1).

Faults observed in line 72-09 (Fig. 9) may be conjugate strike-slip faults. Most are near vertical with small vertical separations. A swarm of left-lateral strike-slip events in 2008 was interpreted to be centered just 10 km to the south of a left lateral offset seen in the gravity anomaly (Bird et al., 2008). Conjugate strike-slip faulting is a common feature ac-commodating shear between overlapping strike-slip faults (e.g., Schreurs, 2003). Rotation of crustal blocks between the QCF and RDF on conjugate strike-slip faults would create small regions of transpression and transtension.

Although the overall tectonic framework is that of trans-pression, there is not a great deal of evidence for compres-sion in the plateau between the RDF and the QCF. Southeast of the southernmost terrace and for a distance of 25 km along the QCF, folds and transpressionally faulted sediments can be seen in the reflection data. For the next 30 km of the fault, sediments tilt down toward the QCF, but tilting could accom-plish a few hundred meters of shortening at most. This tilt is similar to that seen in the Winona basin, but sediments here were estimated to be ~2 s thick next to the QCF (Carbotte et al., 1989) compared to 4 s in the Winona basin (Davis and Riddihough, 1982; Rohr and Tryon, 2010). Such tilt may have been started under transpression and been further ac-centuated by heavy sedimentation during the Pleistocene when this crust was opposite canyons in the shelf edge (Bar-rie and Conway, 1999). However, that tilt alone is not defini-tive evidence of transpression because significant tilt is also observed in extensional stepovers (Christie-Blick and Bid-dle, 1985; Mann, 2007; Rodriguez et al., 2013).

Segmentation

This work interprets that two segments comprise the southernmost QCF: a segment defined by overlap of two strike-slip faults and a more transpressive segment defined by historic pure shear deformation (Fig. 12). To the north, the transpressive segment ends at 53°10′ with a significant change in fault trend (Tréhu et al., 2015; Walton et al., 2015).

Aftershocks of magnitudes greater than 4.5 from the 1949 **M** 8.1 earthquake are considered to have occurred as far south as 52°25′ N (Bostwick, 1984; Rogers, 1986), which is in the vicinity of both the left steps in the QCF and the northern tip of the RDF (Fig. 12). Fault stepovers greater than 5 km can act as barriers to rupture (Graymer et al., 2007; Yıkılmaz et al., 2014). The step is 7 km wide at the location of the highest pop-up structure, showing that the distance between the RDF and QCF appears too large to have allowed rupture to continue southward.

The overlap region is likely the southern limit of the seg-ment of the plate boundary that ruptured in the 2012 M_{w} 7.8 event (Farahbod and Kao, 2015; Kao et al., 2015; Nyko-laishen et al., 2015). The southern extent of the rupture plane is not precisely constrained but is roughly coincident with the northern RDF. Stepovers are often the locus of intense and complex deformation (e.g., Kim et al., 2004).

Observations of structures in the Pacific plate over 400 km adjacent to the QCF (Tréhu et al., 2015) suggest that where the angle of transpression is less than 15°, compres-sion is accommodated through synthetic shears in a simple shear setting. Transpression greater than 15°–20° is required to generate thrust faults parallel to the QCF in a pure shear setting. This change occurs at 53°10′ N (Tréhu et al., 2015; Walton et al., 2015). Combined with results from this article, it is evident that only the plate boundary segment between 52°5′ and 53°10′ N could be in pure shear. This segment is ~100 km long and much, if not most, of a thrust fault within it ruptured in the 2012 M_{w} 7.8 event (James et al., 2013; Lay et al., 2013; Farahbod and Kao, 2015; Kao et al., 2015; Ny-kolaisen et al., 2015). Given the obliquity of the thrust focal mechanism to the relative plate motion (Kao et al., 2015) (Fig. 3), the recent change in orientation of the QCF in this segment may have changed the mode of deformation from pure to simple shear.

Crustal movement in the North American plate follow-ing the 2012 M_{w} 7.8 event differed between the two southern segments. GPS measurements on Haida Gwaii (Nykolaishen et al., 2015) found that postseismic motions inboard of the overlap segment are subparallel to the QCF. In contrast, crust inboard of the transpressive segment moved in expected sympathy to the thrust motion after the earthquake. It may also be significant that a 250–300 m increase in peak height on Moresby Island (Fig. 12) is coincident with the newly defined boundary between these segments. Rocks of the San Cristoval plutonic suite outcrop inboard of both seg-ments so the change in peak height is not the result of erosion of different rock types

Terrace Evolution

Deformation of oceanic basement (Figs. 7 and 8) along the western edge of the plateau indicates that the young Pacific crust has been deformed under transpression of 15° and less. It seems likely that oceanic crust under ~20° of transpression along the QCF would also be deformed and that deformed oceanic crust could underlie the terrace. Refraction studies have interpreted oceanic crustal velocities in a nearly flat layer ~5 km below the seafloor (Horn et al., 1984; Deh-ler and Clowes, 1988), which would be well above the pre-dicted depth of a subducted slab interface. These results have been confirmed by preliminary interpretations of OBS re-fraction data (Riedel et al., 2014). Intraplate deformation may well be an important component of accommodation of transpression (Rohr et al., 2000).

Conclusions

Geomorphology, seismicity, sidescan data, and structures observed in seismic reflection profiles indicate that part of the QCF has propagated incrementally south into a slightly less transpressive configuration and the RDF has propagated north as a bypass fault so that it now overlaps the QCF for 120 km.

The surficial trace of the QCF strikes 5° more clockwise than previously inferred. Southward propagation appears to have been accomplished through a series of sharp left steps and associated bathymetric uplift. This change in fault orientation and the left steps are coincident with the southern limit of aftershocks from the 1949 **M** 8.1 earthquake.

Earthquakes up to M_w 6.4 have been recorded in a zone trending northwest from the previously mapped RDF, coinciding with an oceanic crustal fault and bathymetric uplift. Further along this trend a ridge in the terrace is parallel to the relative plate motions and ends in a depression in the otherwise uplifted Queen Charlotte terrace. Overlap between the RDF and QCF is transtensional, as characterized by recent igneous activity and near-vertical faults that cut young sediments.

Overlap between the QCF and the RDF coincides with a gap in significant earthquake occurrence on the QCF and is distinct from the segment to the north, which is characterized by transpressive deformation of a terrace and flexural trough. The northernmost tip of the RDF disrupts the terrace and marks the southern extent of significant rupture of the 2012 M_w 7.8 thrust earthquake. This revised fault mapping suggests that this segment of the Pacific–North American plate boundary is evolving into a mechanically more efficient configuration.

Data and Resources

Earthquake locations are from the catalog of Earthquakes Canada (April, 2014), Geological Survey of Canada, National Earthquake Database, Earthquake Search (online Bulletin; http://earthquakescanada.nrcan.gc.ca/stndon/NEDB-BNDS /bull-eng.php, last accessed April 2014). Digital scans of Open Files and the sidescan data are available from GEOSCAN, Natural Resources Canada (http://geoscan.nrcan.gc.ca/starweb/ geoscan/servlet.starweb?path=geoscan/geoscan_e.web; last accessed May 2014). Two seismic reflection profiles: F-7-89-EG-56 and F-7-89-EG-58 were downloaded from the National Archive of Marine Seismic Surveys (http://walrus.wr.usgs. gov/NAMSS/; last accessed April 2014).

Acknowledgments

References

Allan, J. F., R. L. Chase, B. Cousens, P. Michael, M. P. Gorton, and S. D. Scott (1993). The Tuzo Wilson volcanic field, NE Pacific: Alkaline volcanism at a complex, diffuse, transform-trench-ridge triple junction, *J. Geophys. Res.* **98,** 22,367–22,387.

Atwater, T., and J. M. Stock (1998). Pacific-North America plate tectonics of the Neogene southwestern United States—An update, *Int. Geol. Rev.* **40,** 375–402.

Barrie, J. V., and K. W. Conway (1999). Late Quaternary glaciation and postglacial stratigraphy of the northern Pacific margin of Canada, *Quat. Res.* **51,** 113–123.

Barrie, V. B., K. W. Conway, and P. T. Harris (2013). Anatomy of a fault: Queen Charlotte fault, British Columbia, Canada, *Geo Mar. Lett.* **33,** 311–318.

Berubé, J., G. C. Rogers, R. M. Ellis, and E. O. Hasselgren (1989). A micro-seismicity study of the Queen Charlotte Island region, *Can. J. Earth Sci.* **26,** 2556–2566.

Bird, A. L. (1997). Earthquakes in the Queen Charlotte region: 1982–1996, *M.Sc. Thesis*, University of Victoria, Victoria, British Columbia, Canada, 125 pp.

Bird, A. L., G. C. Rogers, J. F. Cassidy, H. Kao, H. Dragert, and W. Bentkowski (2008). January 2008 Revere-Dellwood-Wilson fault earthquake sequence offshore British Columbia, *Seismological Society of America Annual Meeting Abstract*, Santa Fe, New Mexico, 16–18 April 2008, http://www.seismosoc.org/meetings/showabstract.php? recid=5518 (last accessed March 2015).

Bostwick, T. K. (1984). A re-examination of the August 22, 1949 Queen Charlotte earthquake, *M.Sc. Thesis*, University of British Columbia, Vancouver, British Columbia.

Braunmiller, J., and J. Nabelek (2002). Seismotectonics of the Explorer region, *J. Geophys. Res.* **107,** doi: 10.1029/2001JB000220.

Bruns, T. R., A. J. Stevenson, and M. R. Dobson (1992). GLORIA investigation of the Exclusive Economic Zone in the Gulf of Alaska and off southeast Alaska: M/V *Farnella* Cruise F7-89-GA, June 14–July 13, 1989, *U.S. Geol. Surv. Open-File Rept. 92-317*, 1–16.

Canadian Hydrographic Services (1983). Queen Charlotte Sound to Dixon Entrance, Chart 3002, scale 1:525,000, http://www.charts.gc.ca/charts-cartes/ paper-papier/index-eng.asp?step=1&by=showChart#=3002#h2 (last accessed March 2015).

Carbotte, S. M., J. M. Dixon, E. Farrar, E. E. Davis, and R. P. Riddihough (1989). Geological and geophysical characteristics of the Tuzo Wilson seamounts: Implications for plate geometry in the vicinity of the Pacific–North America–Explorer triple junction, *Can. J. Earth Sci.* **26,** 2365–2384.

Chase, R. L. (1977). J. Tuzo Wilson Knolls, Canadian hotspot, *Nature* **266,** 344–346.

Chase, R. L., and D. L. Tiffin (1972). Queen Charlotte Fault-Zone, British Columbia, *24th International Geological Congress*, Montreal, Canada, Marine Geology and Geophysics Section 8, 17–28.

Christie-Blick, N., and K. T. Biddle (1985). Deformation and basin formation along strike-slip faults, in Strike-Slip Deformation, Basin Formation, and Sedimentation, K. T. Biddle and N. Christie-Blick (Editors), Society of Economic Paleontologists and Mineralogists, Tulsa, Oklahoma, Special Publication 37, 1–35.

Cousens, B. L., R. L. Chase, and J.-G. Schilling (1985). Geochemistry and origin of volcanic rocks from Tuzo Wilson and Bowie seamounts, northeast Pacific Ocean, *Can. J. Earth Sci.* **22,** 1609–1617.

Davis, E. E., and R. G. Currie (1993). Geophysical observations of the northern Juan de Fuca Ridge system: Lessons in sea-floor spreading, *Can. J. Earth Sci.* **30,** 278–300.

Davis, E. E., and R. P. Riddihough (1982). The Winona basin: Structure and tectonics, *Can. J. Earth Sci.* **19,** 767–788.

Davis, E. E., and D. A. Seemann (1981). A compilation of seismic reflection profiles across the continental margin of western Canada, *Geol. Surv. of Can. Open-File Rept. 751*, Vancouver, British Columbia, Canada.

Davis, E. E., R. G. Currie, and B. Sawyer (1987a). Acoustic imagery, southern Queen Charlotte margin, *Geological Survey of Canada, Preliminary Map 10-1987*, 1 sheet, doi: 10.4095/133936.

Davis, E. E., R. G. Currie, and B. Sawyer (1987b). Acoustic imagery, Wilson/Dellwood Knolls, *Geological Survey of Canada, Preliminary Map 11-1987*, 1 sheet, doi: 10.4095/133937.

Dehler, S. A., and R. M. Clowes (1988). The Queen Charlotte Islands refraction project, part I, The Queen Charlotte fault zone, *Can. J. Earth Sci.* **25,** 1857–1870.

DeMets, C., R. G. Gordon, and D. F. Argus (2010). Geologically current plate motions, *Geophys. J. Int.* **181,** 1–80, doi: 10.1111/j.1365-246X.2009.04491.x.

DeMets, C., R. G. Gordon, D. F. Argus, and S. Stein (1994). Effect of recent revision to the geomagnetic reversal time scale on estimates of current plate motions, *Geophys. Res. Lett.* **21,** 2191–2194.

Doubrovine, P. V., and J. A. Tarduno (2008). A revised kinematic model for the relative motion between Pacific oceanic plates and North America since the Late Cretaceous, *J. Geophys. Res.* **113,** no. B12101, doi: 10.1029/2008JB005585.

Farahbod, A., and H. Kao (2015). Spatiotemporal distribution of events during the first week of the 2012 Haida Gwaii aftershock sequence, *Bull. Seismol. Soc. Am.* **105,** no. 2B, doi: 10.1785/0120140173.

Graymer, R. W., V. E. Langenheim, R. W. Simpson, R. C. Jachens, and D. A. Ponce (2007). Relatively simple through-going fault planes at large-earthquake depth may be concealed by the surface complexity of strike-slip faults, in *Tectonics of Strike-Slip Restraining and Releasing Bends*, D. Cunningham and P. Mann (Editors), Geological Society of London, London, United Kingdom, Special Publication 290, 189–201.

Horn, J. R., R. M. Clowes, R. M. Ellis, and D. N. Bird (1984). The seismic structure across an active oceanic/continental transform fault zone, *J. Geophys. Res.* **89,** 3107–3120.

Hyndman, R. D., and R. M. Ellis (1981). Queen Charlotte fault zone: Microearthquakes from a temporary array of land stations and ocean bottom seismographs, *Can. J. Earth Sci.* **18,** 776–788.

Hyndman, R. D., and T. S. Hamilton (1993). Queen Charlotte area Cenozoic tectonics and volcanism and their association with relative plate motions along the northeastern Pacific margin, *J. Geophys. Res.* **98,** 14257–14277.

Hyndman, R. D., T. J. Lewis, J. A. Wright, M. Burgess, D. S. Chapman, and M. Yamano (1982). Queen Charlotte fault zone: Heat flow measurements, *Can. J. Earth Sci.* **19,** 1657–1669, doi: 10.1139/e82-141.

Hyndman, R. D., R. P. Riddihough, and R. Herzer (1979). The Nootka fault zone, *Geophys. J. Roy. Astron. Soc.* **58,** 667–683.

Hyndman, R. D., G. D. Spence, T. Yuan, and E. E. Davis (1994). Regional geophysics and structural framework of the Vancouver Island margin accretionary prism, in G. K. Westbrook, C. Bobb, and R. J. Musgrave (Editors), *Proc. of the Ocean Drilling Program, Initial Reports*, Ocean Drilling Program, Vol. 146, Part 1, College Station Texas, 399–419, http://www-odp.tamu.edu/publications/146_1_IR/VOLUME/CHAPTERS/ir146pt1_10.pdf (last accessed March 2015).

James, T., G. Rogers, J. Cassidy, H. Dragert, R. Hyndman, L. Leonard, L. Nykolaishen, M. Riedel, M. Schmidt, and K. Wang (2013). Field studies target 2012 Haida Gwaii earthquake, *Eos Trans. AGU* **94,** 197–198.

Kao, H., S.-J. Shan, A. Bent, C. Woodgold, G. Rogers, J. F. Cassidy, and J. Ristau (2012). Regional centroid-moment-tensor analysis for earthquakes in Canada and adjacent regions: An update, *Seismol. Res. Lett.* **83,** 505–515, doi: 10.1785/gssrl.83.3.505.

Kao, H., S.-J. Shan, and A. Farahbod (2015). Source characteristics of the 2012 Haida Gwaii earthquake sequence, *Bull. Seismol. Soc. Am.* **105,** no. 2B, doi: 10.1785/0120140165.

Kim, Y.-S., D. C. P. Peacock, and D. J. Sanderson (2004). Fault damage zones, *J. Struct. Geol.* **26,** 503–517.

Lay, T., L. Ye, H. Kanamori, Y. Yamazaki, K. F. Cheung, K. Kwong, and K. D. Koper (2013). The October 28, 2012 M_w 7.8 Haida Gwaii underthrusting earthquake and tsunami: Slip partitioning along the Queen Charlotte fault transpressional plate boundary, *Earth Planet. Sci. Lett.* **375,** 57–70.

Mann, P. (2007). Global catalogue, classification and tectonic origins of restraining- and releasing bends on active and ancient strike-slip fault systems, in *Tectonics of Strike-Slip Restraining and Releasing Bends*, D. Cunningham and P. Mann (Editors), Geological Society of London, London, United Kingdom, Special Publication 290, 13–142, doi: 10.1144/SP290.2.

Nykolaishen, L., H. Dragert, K. Wang, T. James, and M. Schmidt (2015). GPS observations of crustal deformation associated with the M_w 7.8 Haida Gwaii earthquake, *Bull. Seismol. Soc. Am.* **105,** no. 2B, doi: 10.1785/0120140177.

Riedel, M., M. Côté, P. Neelands, G. Middleton, G. Standen, R. Iuliucci, M. Ulmi, C. Stacey, R. Murphy, D. Manning, *et al.* (2014). 2012 Haida Gwaii M_w 7.7 earthquake response—Ocean bottom seismometer relocation and geophone orientation analysis and quality control of wide-angle P-wave refraction data, *Geol. Surv. Can. Open-File Rept. 7632,* 1–79.

Ristau, J. R., G. C. Rogers, and J. F. Cassidy (2007). Stress in western Canada from regional moment tensor analysis, *Can. J. Earth Sci.* **44,** 127–150.

Rodriguez, M., N. Chamot-Rooke, M. Fournier, P. Huchon, and M. Delescluse (2013). Mode of opening of an oceanic pull-apart: The 20° N basin along the Owen fracture zone (NW Indian Ocean), *Tectonics* **32,** 1–15, doi: 10.1002/tect.20083.

Rogers, G. C. (1986). Seismic gaps along the Queen Charlotte fault, *Earthq. Predic. Res.* **4,** 1–11.

Rohr, K. M. M., and L. Currie (1997). Queen Charlotte basin and Coast Mountains: Paired belts of subsidence and uplift caused by a low-angle normal fault, *Geology* **25,** 819–822.

Rohr, K. M. M., and J. R. Dietrich (1992). Strike slip tectonics and development of the Tertiary Queen Charlotte basin, offshore western Canada: Evidence from seismic reflection data, *Basin Res.* **4,** 1–20, doi: 10.1111/j.1365-2117.1992.tb00039.x.

Rohr, K. M. M., and K. P. Furlong (1995). Ephemeral plate tectonics at the Queen Charlotte triple junction, *Geology* **23,** 1035–1038.

Rohr, K. M. M., and A. J. Tryon (2010). Pacific-North America plate boundary reorganization in response to a change in relative plate motion: Offshore Canada, *Geochem. Geophys, Geosyst.* **11,** Q06007, doi: 10.1029/2009GC003019.

Rohr, K. M. M., M. Scheidhauer, and A. M. Tréhu (2000). Transpression between two warm mafic plates: The Queen Charlotte fault revisited, *J. Geophys. Res.* **105,** 8147–8172.

Schreurs, G. (2003). Fault development and interaction in distributed strike-slip shear zones: An experimental approach, in *Intraplate Strike-Slip Deformation Belts*, F. Storti, R. E. Holdsworth, and F. Salvini (Editors), Geological Society, London, United Kingdom, Special Publication 210, 35–52.

Shaw, J. H., C. Connors, and J. Suppe (2005). Structural interpretation methods, in *Seismic Interpretation of Contractional Fault-Related Folds: An AAPG Seismic Atlas*, J. H. Suppe, C. Shaw, and J. Connors (Editors), American Association Petroleum Geologists, Tulsa Oklahoma, Studies in Geology 53, 2–58.

Smith, A. J., R. D. Hyndman, J. F. Cassidy, and K. Wang (2003). Structure, seismicity and thermal regime of the Queen Charlotte transform margin, *J. Geophys. Res.* **108,** 2539, doi: 10.1029/2002JB002247.

Sykes, L. R. (1971). Aftershock zones of great earthquakes, seismicity gaps and earthquake prediction for Alaska and the Aleutians, *J. Geophys. Res.* **76,** 8021–8041.

Tréhu, A. M., M. Scheidhauer, K. M. M. Rohr, B. Tikoff, M. A. L. Walton, S. P. S. Gulick, and E. C. Roland (2015). An abrupt transition in the mechanical response of the upper crust to transpression across the Queen Charlotte fault, *Bull. Seismol. Soc. Am.* **105,** no. 2B, doi: 10.1785/0120140159.

Wakabayashi, J., J. V. Hengesh, and T. L. Sawyer (2004). Four-dimensional transform fault processes: Progressive evolution of step-overs and bends, *Tectonophysics* **392,** 279–301.

Walton, M.A.L., S. P. S. Gulick, E. C. Roland, P. J. Haeussler, and A. M. Tréhu (2015). Basement and regional structure along-strike of the Queen

Charlotte fault in the context of modern and historical earthquake ruptures, *Bull. Seismol. Soc. Am.* **105,** no. 2B, doi: 10.1785/0120140174.

Wilcox, R. E., T. P. Harding, and D. R. Seely (1973). Basin wrench tectonics, *Am. Assoc. Petrol. Geol. Bull.* **57,** 74–96.

Wilson, D. S. (1988). Tectonic history of the Juan de Fuca ridge over the last 40 million years, *J. Geophys. Res.* **93,** 11,863–11,876, doi: 10.1029/JB093iB10p11863.

Wilson, D. S. (2002). The Juan de Fuca plate and slab: Isochron structure and Cenozoic plate motions, in *The Cascadia Subduction Zone and Related Subduction Systems*, S. Kirby, K. Wang, and S. Dunlop (Editors), *Geol. Surv. Canada Open-File Rept. 4350*, Vancouver, British Columbia, 9–12.

Yıkılmaz, M. B., D. L. Turcotte, E. M. Heien, L. H. Kellogg, and J. B. Rundle (2014). Critical jump distance for propagating earthquake ruptures across step-overs, *Pure Appl. Geophys.*, doi: 10.1007/s00024-014-0786-y.

Kristin Rohr Consulting
719 Birch Road
N. Saanich, British Columbia
V8L 5S1 Canada